Princeton Plasma Physics Laboratory

PPPL- 4386

PPPL- 4386

Relationship Between Onset Thresholds, Trigger Types, and Rotation Shear for the m/n=2/1 Neoclassical Tearing Mode in a High-β Spherical Torus

S.P. Gerhardt, D.P. Brennan, R. Buttery, R.J. La Haye, S. Sabbagh, E. Strait,
M. Bell, R. Bell, E. Fredrickson, D. Gates, B. LeBlanc, J. Menard,
D. Stutman, K.Tritz, and H. Yuh

February, 2009

Prepared for the U.S. Department of Energy under Contract DE-AC02-76CH03073.

Princeton Plasma Physics Laboratory
Report Disclaimers

PPPL Report Availability

Princeton Plasma Physics Laboratory:

http://www.pppl.gov/techreports.cfm

Office of Scientific and Technical Information (OSTI):

http://www.osti.gov/bridge

Related Links:

U.S. Department of Energy

Office of Scientific and Technical Information

Fusion Links

Relationship between onset thresholds, trigger types, and rotation shear for the m/n=2/1 neoclassical tearing mode in a high-β spherical torus

S.P. Gerhardt[1], D.P. Brennan[2], R. Buttery[3], R. J. La Haye[4], S. Sabbagh[5], E. Strait[4], M. Bell[2], R. Bell[1], E. Fredrickson[1], D. Gates[1], B. LeBlanc[1], J. Menard[1], D. Stutman[6], K. Tritz[6], H. Yuh[7]

[1] Princeton Plasma Physics Laboratory, Princeton, New Jersey, USA
[2] University of Tulsa, Tulsa, Oklahoma, USA
[3] EURATOM/UKAEA Fusion Association, Culham Science Centre, Abingdon, Oxon, OX14 3DB, United Kingdom
[4] General Atomics, P.O. Box 85608, San Diego, California 92186-5608, USA
[5] Columbia University, New York, New York, USA
[6] The Johns Hopkins University, Baltimore, Maryland, USA
[7] Nova Photonics, Princeton, New Jersey, USA

Abstract The onset conditions for the m/n=2/1 neoclassical tearing mode (NTM) are studied in terms of neoclassical drive, triggering instabilities, and toroidal rotation or rotation shear, in the spherical torus NSTX [M. Ono, et al., Nuclear Fusion **40**, 557 (2000)]. There are three typical onset conditions for these modes, given in order of increasing neoclassical drive required for mode onset: triggering by energetic particle modes, triggering by edge localized modes, and cases where the modes appear to grow without a trigger. In all cases, the required drive increases with toroidal rotation shear, implying a stabilizing effect from the shear.

PACS #s: 52.35.Py, 52.55.Fa

1: Introduction

The neoclassical tearing mode (NTM) [1] is a beta-limiting instability in tokamaks: when a magnetic island forms, rapid parallel transport causes pressure flattening across the magnetic island, leading to a reduction in the pressure driven bootstrap current which then further increases the island size. NTMs are likely to be a dominant performance limiting instability in large tokamaks like ITER if mitigation techniques are not implemented [2]. Experimental results in NSTX and MAST [3] show that these modes also exist in a spherical torus (ST) [4] despite more favorable field-curvature effects [5], and must be accounted for in ST performance predictions as well.

There are many issues in extrapolating our present understanding to larger and more slowly rotating plasmas, either at conventional aspect-ratio or in a ST, two of which are addressed in this letter: i) what instabilities can trigger the nominally metastable NTM, and ii) what is the role of rotation or rotation shear in setting the onset threshold? With regard to triggers, many advanced operational scenarios in the ST or conventional tokamak rely on sawtooth avoidance (with q_{min}>1) or control [6] to avoid triggering these modes; however, other modes such as fish-bones [7] or edge localized modes (ELMs) [8] have been seen to trigger NTMs in conventional aspect ratio tokamaks. With regard to rotation, its role in setting the 2/1 NTM onset threshold in DIII-D was presented in Ref. [8], which utilized that device's unique ability to control the plasma rotation through the co-/counter- neutral beam injection mix. It was found that with all other parameters fixed, the value of β_N ($\beta_N=\beta a B_T/I_P$) at mode onset was reduced as the plasma rotation slowed. While data analysis indicated that the toroidal rotation shear at q=2, rather than the rotation magnitude, was likely the relevant parameter, the strong co-linearity between rotation

and rotation shear made it difficult to separate the relative contributions. It is the purpose of the present letter to describe similar experiments in the National Spherical Torus Experiment (NSTX) [9], where analysis of a large number of discharges allows the demonstration that flow shear plays the important role in influencing the 2/1 onset threshold.

2: Definitions and data set selection

The formulation in the NTM problem in this letter is based on the Modified Rutherford Equation (MRE) [10], which describes the time evolution of a width w island, with r_s the radius of the resonant surface and $\tau_R=\mu_0 r_s^2/1.22\eta_{neo}$ (η_{neo} is the neoclassical resistivity):

$$\frac{\tau_R}{r_s^2}\frac{dw}{dt}=\Delta'+\frac{C_{BS}\mu_0 L_q}{B_\theta}\delta j_{BS}\left(\frac{w}{w^2+w_d^2}-\frac{ww_{pol}^2}{w^4+w_b^4}\right)-\frac{6D_R}{\sqrt{w^2+0.2w_d^2}} \quad (1)$$

Here, Δ' is the classical tearing stability index [11]. The term proceeding the parenthesis represents the drive due to the lost bootstrap current (δj_{BS}) inside the magnetic island. For the analysis described here, the missing bootstrap current is calculated from the formulas in Ref. [12] as

$$\delta j_{BS,Sauter}=\frac{I(\psi)p_e\left(L_{31}\frac{1}{p_e}\frac{dp_e}{d\psi}+L_{32}\frac{1}{T_e}\frac{dT_e}{d\psi}\right)}{\sqrt{\langle B^2\rangle}}\ , \quad (2)$$

where the terms $I(\psi)$, L_{31}, and L_{32} are defined in that reference, p_e and T_e are the electron pressure and temperature, and ψ is poloidal flux. Defining the drive as $\frac{\mu_0 L_q \delta j_{BS}}{B_\theta}$, compared to the global β_N or local β_P, is a more accurate representation of the local NTM physics when discharges with varying profiles are compared, provided that high-quality equilibrium calculations exist. The D_R term represents the stabilizing effects of field line curvature [1].

The terms w_d, w_{pol}, and w_b describe stabilizing effects relevant for small islands (see Ref [1] and references therein). Of particular interest in this rotation-oriented study is the w_{pol} term, a characteristic size for the polarization current effect [13] given by:

$$w_{pol}^2 \propto \rho_{i,\theta}^2\frac{\Omega\left(\Omega-\omega_i^*\right)}{\omega_e^{*2}} \quad (3)$$

Here, $\Omega=\omega_{Mirnov}-\omega_{Er=0}$ is the frequency of the mode in the $E_r=0$ frame and $\omega_{e,i}^*$ are the diamagnetic drift frequencies of electrons and ions (see Ref. [14] for details and definitions). This term is predicted to be stabilizing for $0<\Omega<\omega_i^*$, but destabilizing in the regime $\Omega<0$, indicating a means for rotation to impact the stability at onset.

Rotation can enter the NTM problem through three additional routes [8]: i) the absolute value of toroidal rotation may play a role through coupling to error fields and the resistive wall, ii) differential rotation between surfaces can modify coupling to triggers and iii) both rotation shear and differential rotation may modify the classical tearing stability, through either Δ' or inner-layer effects. Here, the normalized toroidal rotation shear is defined as $-2\pi L_s\tau_A(dF_T/dr)$ [15], where F_T is the toroidal rotation frequency in Hz, $L_s=qL_q/\varepsilon$, $L_q=q/(dq/dr)$, ε is the difference in magnetic fields strengths between the inboard and outboard midplane normalized to their sum, $\tau_A=R_0(\mu_0 m_i n_i)^{1/2}/B_{T0}$ with R_0 the geometric axis, B_{T0} the vacuum toroidal field on axis, and m_i and n_i the ion mass and number density, and $r=a\sqrt{\frac{\psi-\psi_{edge}}{\psi_{axis}-\psi_{edge}}}$ with a the minor radius.

The results presented here come from high-elongation (κ), high-triangularity (δ) lower-single-null plasmas, heated by neutral beams injecting parallel to the plasma current, and

satisfying the following parameters: 900kA<I_P (plasma current)<1000kA, 2.1<κ<2.4, 0.6<δ<0.8, 0.55<l_i (internal inductance)<0.8, 4<P_{inj} (injected power, MW) <6.5. Furthermore, the collisionality, defined as $\nu_i^* = \frac{520 n_e (10^{19} m^{-3}) Rq}{\varepsilon^{3/2} T_i^2 (eV)}$ [16], is limited to the range 0.05< ν_i *<0.1. There are no sawteeth, with q_{min} greater than, but approaching, 1 through the discharge; 2/1 modes triggered by sawteeth have not been observed, though this may result simply from the general avoidance of sawtoothing discharges due to the rapid flux consumption in those cases. A large variety of rotation profiles are present in the 47 shot database, due to a wide range of applied non-resonant magnetic field n=3 rotation braking [17] and varying neutral beam input powers.

3: Examples of triggers

A common set of features distinguish these n=1 modes in NSTX. Although the mode frequency immediately at onset may not match the q=2 rotation frequency inferred from charge exchange spectroscopy and equilibrium reconstruction, the two frequencies quickly approach each other and the saturated mode frequency closely tracks the q=2 rotation frequency thereafter. Flat spots become visible in the electron temperature profile at the q=2 surface, and in the fully evolved state, the initially peaked rotation profile becomes flat inside of q=2.

There are, however, multiple mechanisms responsible for the onset of the mode. NTM growth has been observed in NSTX from at least three mechanisms: chirping energetic particle modes (EPMs), ELMs, and "triggerless" cases where the mode grows with no discernable trigger. Examples of each case are illustrated in Fig 1, where each column corresponds to a different discharge and trigger type. The spectrograms in the top row are computed from the frequency content of a single Mirnov coil signal, while the toroidal mode number identification is done by phase analysis of toroidally separated coils. The mode amplitude evolution in the middle row is determined by following the zero-crossings of the filtered difference of two Mirnov coils separated toroidally by 180°, i.e. discrimination for odd-n pickup. The bottom row shows the divertor D_α emission and D-D neutron emission, along with the value of β_N at mode onset; the no-wall n=1 β_N limit is typically in the range 3.8-4 for this class of discharges.

The first column shows an example EPM trigger case. A series of sharp neutron-rate drops is visible near t=0.56, indicative of the rapid loss of fast ions, and a weakly growing mode is apparent at t=0.58, though it dies away. The final 2/1 mode strikes at t=0.605 seconds, coincident with a final rapid drop in the D-D neutron rate. The spectrogram for this example shows that chirping n=1 & 2 fishbone modes are present at each of the neutron-rate drops. These chirps are extremely rapid, taking approximately 1 msec. in total. In the case of the triggering mode, it appears that an n=1 mode chirps down to ~14 kHz, i.e. slightly below the core rotation frequency, while the 2/1 mode then grows from at or just slightly under then 2/1 surface rotation frequency. Analysis of the soft X-ray data is missing for this discharge; however, it is typical to find a core perturbation with odd parity across the magnetic axis during these chirps. This is the signature of a 1/1 mode, and it is possible that toroidal coupling of the 1/1 mode drives a seed island at the 2/1 surface; however, the rapid nature of the interaction obscures the details. Note that n=1 fishbones have been observed in NSTX even in the absence of a q=1 surface [18].

The center column of figures shows a case where the mode is triggered by the ELM at 0.54 sec. When it first strikes, the mode frequency is significantly less than the q=2 rotation frequency, as might be anticipated when the trigger-perturbation comes from the plasma edge. It is likely that the ELMs have a broad spectrum, including an n=1 component than can couple to the 2/1 surface and drive the seed island; these perturbations are quite transient, however, and are not resolved with the Fourier analysis techniques utilized in this paper. These modes often grow from very low amplitude; the presence of a large ELM at the onset time and the low initial mode frequency are the distinguishing feature of this onset mechanism. Note that due to the small size

of the seed islands in these cases, it is possible that these are examples of "mixed seeding" [19], where the modes are weakly linearly unstable at onset, but the initial island is provided by another instability.

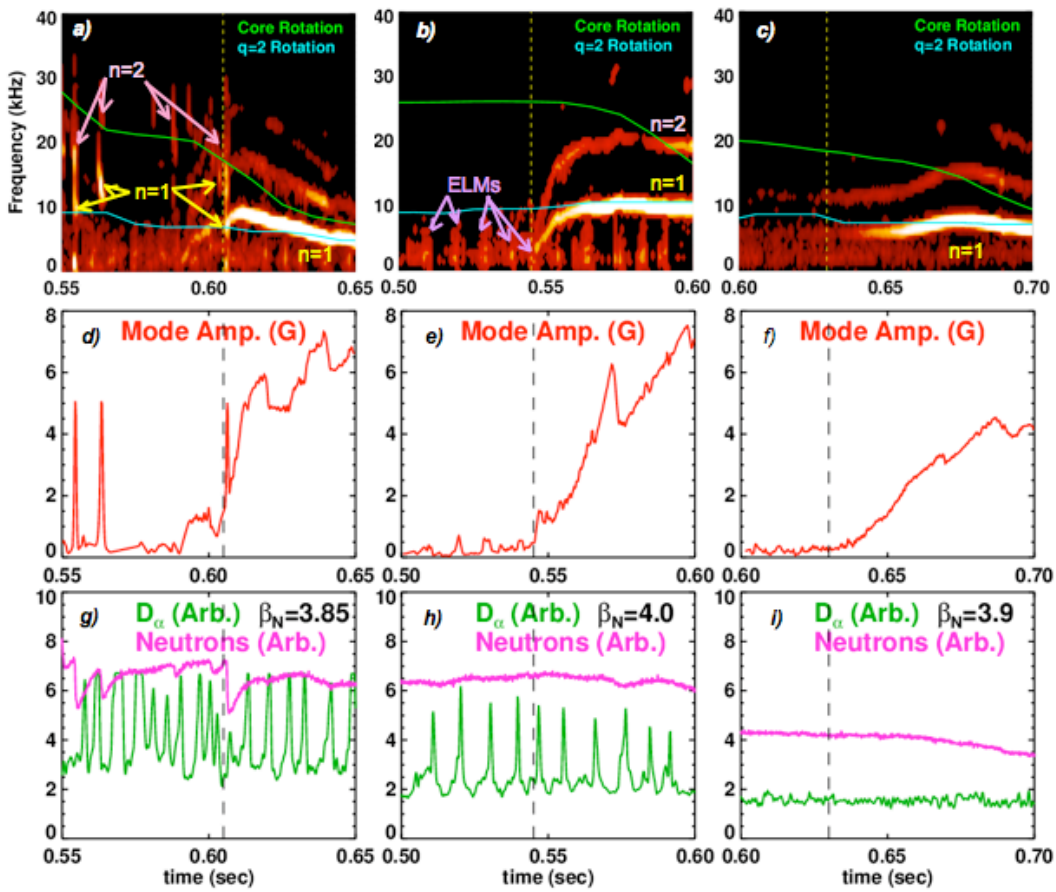

Fig 1.Time traces and spectrograms of typical triggers. Each column corresponds to a single discharge, with an EPM triggered case on the left, an ELM triggered case in the center, and case with no visible trigger on the right. The upper row shows single-coil spectrograms for each case, where the mode numbers have been determined by phase analysis from toroidally separate coils, the middle row shows the mode amplitude, and the lowest row shows the divertor D_α and neutron emission.

The right column illustrates a case where there are no clear NTM triggers present. Both the D_α and neutron emission show no features when the mode strikes, and there are no trigger signatures on the multi-chord ultra-soft X-ray (USXR) system. In addition to the lack of any visible perturbation, the modes in these cases always grow with an initial frequency near to that of the q=2 surface rotation. NTMs without a trigger have been observed in the past [7, 20, 21]; a likely yet untested hypothesis in the present case is that the modes are linearly unstable at onset.

The mode eigenfunction has been studied with the 30-chord USXR detector system. This system typically sees the inversion layer associated with the magnetic island, and use of a 2/1 island model and the inverted USXR data is capable of reproducing the measured emission fluctuations from chords whose tangency radius is near q=2. However, the emission from the plasma core is typically inconsistent with a pure even-m eigenfunction (for instance, the measured emission is odd across the magnetic axis), implying the presence of a coupled odd-m mode, likely 1/1. Any effect of this inner mode on the 2/1 mode stability is not reflected in an

analysis based on equation 1. Note that the coupling of m/n NTMs to m-1/n modes has been observed in TFTR [20] and ASDEX-Upgrade [7], and predicted by theory [22].

4: Onset threshold vs. rotation and trigger type

As noted in Sect. 2, the mode frequency at onset may be an important parameter in determining the onset threshold. Fig. 2a) illustrates this initial mode frequency, compared to the toroidal rotation frequency of the q=2 surface. When the mode is triggered by an ELM, the mode frequency at onset is always significantly slower than the q=2 surface rotation frequency. The cases with EPM triggers can rotate either faster or slower than the q=2 surface. Those cases with no visible triggers are typically observed to grow with a frequency only slightly less than the q=2 surface rotation. For reference, the inset in Fig. 2a) shows the mode and q=2 surface rotation frequencies at a later time, when the mode amplitude has saturated; the frequency match is then quite good.

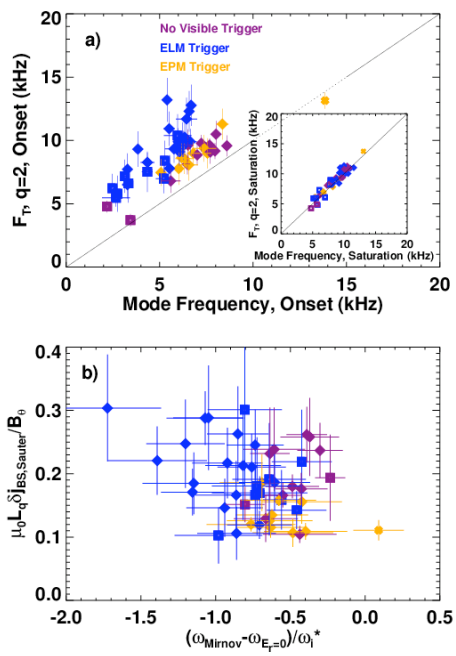

Fig 2. a) Mode frequency at onset compared to the q=2 surface rotation frequency at onset, with a similar figure for the mode frequency at saturation in the inset, and b) the mode frequency in the E_r=0 frame, normalized to the ion-diamagnetic drift frequency.

Given that the modes most often travel more slowly than the q=2 surface and the arguments in Sect. 2, it appears that the polarization term might be a candidate for providing a rotation dependence in the onset drive. The method used here to assess this physics is essentially that in Ref. [14]. The rotation frequency of the E_R=0 frame is calculated as

$$\omega_{E_R=0} = -\frac{nV_{\phi,C^{6+}}}{R} + \frac{n}{RZ_{C^{6+}}en_{C^{6+}}B_\theta}\frac{dp_{C^{6+}}}{dr}, \tag{4}$$

where the density, temperature, and pressure of fully ionized carbon are measured with charge exchange spectroscopy (note that poloidal rotation measurements are not available for this dataset). The NTM-drive at onset is plotted against the normalized E_R=0 frame rotation in Fig. 2b); if this were the important physics in setting the mode onset, we would expect that the

required NTM drive would be less at the more negative normalized rotation. However, neither this nor any other trend is observed, and we infer that ion-polarization effects do not play a role in determining the rotation dependence of the onset threshold (a similar observation was made on DIII-D [8]).

Next, consider the possibility that the absolute rotation magnitude modifies the onset threshold. The NTM drive at mode onset is plotted against the q=2 rotation frequency in Fig. 3a. Also indicated in the figure are linear regression coefficients, used as a measure of the trend. In this case, the dataset as a whole shows no trend (r^2=0.1); only the ELM triggered modes show any correlation of the onset drive with rotation magnitude. These and other correlation coefficients are given in Table #1 for comparison.

	All Cases	EPM Triggered	ELM Triggered	"Triggerless"
F_T @ q=2	0.09	0.05	0.40	0.00
$-dF_T/dr$ @ q=2	0.07	0.01	0.15	0.02
$-2\pi L_s\tau_A(dF_T/dr)$	**0.45**	**0.61**	**0.61**	**0.42**
$\tau_A^{2/5}\,\tau_R^{3/5}\,(F_{T,q=2}-F_{T,q=3})$	0.19	0.00	0.42	0.18
$\tau_A^{2/5}\,\tau_R^{3/5}\,(F_{T,q=2}-F_{T,Ped})$	---	---	0.40	---
Best Fit Line Slope	**----**	0.16±0.05	0.2±0.04	0.26±0.09

Table #1, Statistical analysis of the dependence of the NTM onset threshold on rotation, rotation shear, and differential rotation. All numbers are correlation coefficients r^2, except for the final row, which gives the slopes of the best-fit lines in Fig. 3b.

However, a correlation becomes immediately clear, and improved for each onset mechanism or the dataset as a whole, when the onset drive is plotted against rotation shear as in Fig 3b). This conclusion is reinforced by the correlation coefficients in Table #1, where the correlation with normalized flow shear is clearly best. Furthermore, the data and linear fits reveal that for fixed flow shear, the EPM cases in orange are typically triggered at lower values of bootstrap drive. The ELM triggered cases in blue are triggered at intermediate levels of drive, and the "triggerless" cases in purple typically occur at the highest drive levels. There is significantly more scatter for the "triggerless" cases, possibly due to effects not related to rotation shear such as proximity to the ideal kink limit [21] or q_0 to 1 [22]; however, even in this case, the correlation is better with rotation shear than rotation. The slopes of the best-fit lines (Table #1, bottom row) are, to within admittedly large error bars, equal, implying that rotation shear is not entering directly through the triggering physics, and must therefore be influencing the underlying tearing stability. Importantly, *both* the trigger type and rotation-shear effects are important in discerning the underlying trend.

Some simulations and measurements of tearing-mode onset in the presence of flow shear have indicated that differential rotation between adjacent rational surfaces [23] can be stabilizing, or that differential rotation with respect to the triggering surface reduces the seed island size. The onset NTM drive data above has been analyzed as a function of the differential rotation between q=2 and both the q=3 surface and, for the ELM triggered modes, the top of the pedestal (the differential rotation is normalized to the tearing time as per Ref. [1]). These results are also included in table #1, and it is clear that none of these measures are as clearly correlated with the onset drive as the local normalized rotation shear.

A more promising explanation of these results lies in possible stabilizing effects on the classical tearing stability due to flow shear. In slab geometry, flow shear has been found to be either stabilizing or destabilizing, depending on its magnitude relative to magnetic shear [24,25] and the plasma viscosity [26,27]. A similar result was found for cylindrical plasmas with axial flow shear [28], where negative flow shear could be stabilizing in the presence of viscosity. A

second cylindrical geometry study [29] also showed that flow shear (helical flow in this case) could modify the tearing outer-region, leading to stability or instability depending on the flow profile. Finally, a heuristic model for the effect of flow shear interacting with magnetic shear is given in Ref. [15], where the stabilizing effect of magnetic shear is enhanced by flow shear; it is this model which gives rise to the $L_s\tau_A$ normalization used in this letter. Comparing the 2nd and 3rd lines of table #1 indeed shows that this normalization to the flow shear is critical in achieving a good correlation, and enhances this explanation of the experimental results presented here. Note, however, that none of these theories or simulations match the profiles and geometry of the NSTX plasmas; further theoretical and/or computational work is necessary to fully explain these results.

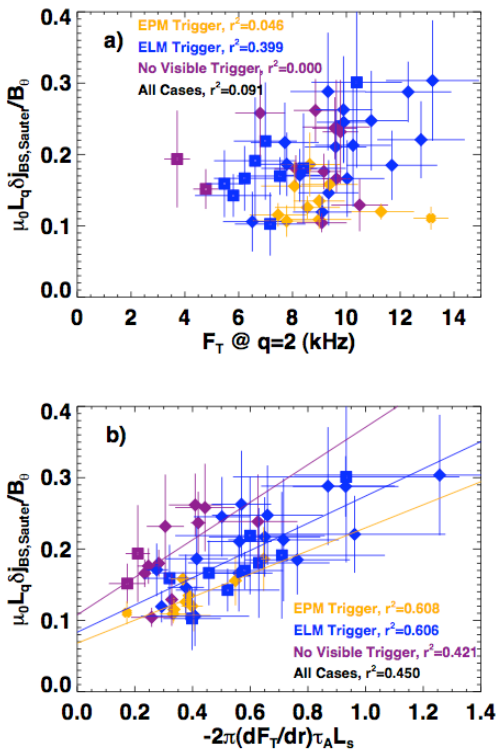

Fig 3. Onset bootstrap drive at mode onset vs. a) rotation and b) rotation shear. Linear correlation coefficients (r^2) are indicated in each frame, sorted by trigger type.

5: Conclusions

The present results demonstrate multiple mechanisms that can lead to 2/1 NTM onset in a spherical torus. For fixed rotation shear, energetic particle modes can trigger NTMs at lower values of NTM drive, while ELMs lead to mode onset at intermediate values; triggerless modes typically, but not always, begin to grow at the highest drive values. Importantly, the inclusion of a wide variety of discharges, including many with magnetic braking, allows the roles of rotation and rotation shear to be separated. Within each subset of trigger types, it is shown that the required NTM drive at onset, and thus the intrinsic stability, increases with increasing rotation shear, but is not strongly correlated with either the absolute magnitude of rotation or the rotation in the E_R=0 frame. These results are the clearest evidence yet that rotation shear-plays an important role in determining the 2/1 NTM onset threshold, probably through the role of the classical tearing stability in governing mode onset.

6: Acknowledgements

This research was funded by the United States Department of Energy. R. Buttery was jointly funded by the UK Engineering and Physical Sciences Research Council and the European Communities.

7: References

[1] R.J. La Haye, Phys. Plasmas **13**, 055501 (2006).
[2] T.C. Hender, et al, Nuclear Fusion **47**, S128 (2007).
[3] R. J. Buttery, et al, Phys. Rev. Lett **88**, 125005 (2002).
[4] Y.K.M. Peng and D.J. Strickler, Nuclear Fusion **26**, 769 (1986)
[5] S. Kruger, C.C. Hegna, and J.D. Callen, Phys. Plasmas **5**, 455 (1998)
[6] O. Sauter, et al., Phys. Rev. Lett **88**, 105001 (2002).
[7] A. Gude, S. Guenter, S. Sesnic, and the ASDEX Upgrade Team, Nuclear Fusion **39**, 127 (1999).
[8] R. J. Buttery, et al, Phys. Plasmas **15**, 056115 (2008)
[9] M. Ono, et al., Nuclear Fusion **40**, 557 (2000).
[10] P.H. Rutherford, Phys. Fluids **16**, 1903 (1973).
[11] H. P. Furth, J. Killeen, and M.N. Rosenbluth, Phys. Fluids **6**, 459 (1963).
[12] O. Sauter, C. Angioni, and Y.R. Lin-Liu, Phys. Plasmas **6**, 2834 (1999).
[13] H.R. Wilson, et al., Plasma Phys. Control. Fusion **38**, A149 (1996).
[14] R. J. La Haye, C. C. Petty, E. J. Strait, F. L. Waelbroeck, and H. R. Wilson, Phys. Plasmas **10**, 3644 (2003).
[15] R.J. La Haye, *The stabilizing effect of flow shear on m/n=3/2 magnetic island width in DIII-D*, submitted to Physics of Plasmas.
[16] T.C. Hender, et al, Nuclear Fusion **44**, 788 (2004).
[17] W. Zhu, et al., Phys. Rev. Lett **96**, 225002 (2006)
[18] E. Fredrickson, L. Chen, and R. White, Nuclear Fusion **43**, 1258 (2003)
[19] D. Brennan, S. E. Kruger, T.A. Gianakon, and D.D. Schnack, Nuclear Fusion **45**, 1178 (2005).
[20] E. Fredrickson, Phys. Plasmas **9**, 548 (2002).
[21] D. Brennan, et al., Phys. Plasmas **10**, 1643 (2003).
[22] D. Brennan, et al., Phys. Plasmas **14**, 06108 (2007).
[23] D. Chandra, A. Sen, P. Kaw, M.P. Bora, and S. Kruger, Nuclear Fusion **45**, 524 (2005).
[24] G. Einaudi and F. Rubini, Phys. Fluids **29**, 2563 (1986).
[25] X.L. Chen and P.J. Morrison, Phys. Fluids B **2**, 495 (1990).
[26] G. Einaudi and F. Rubini, Phys. Fluids B**, 1**, 2224 (1989).
[27] X.L. Chen and P.J. Morrison, Phys. Fluids B **2**, 2574 (1990).
[28] R. Coelho and E. Lazzaro, Phys. Plasmas **14**, 012101 (2007).
[29] D. Chandra, A. Sen, and P. Kaw, Nuclear Fusion **47**, 1238 (2007).

The Princeton Plasma Physics Laboratory is operated
by Princeton University under contract
with the U.S. Department of Energy.

Information Services
Princeton Plasma Physics Laboratory
P.O. Box 451
Princeton, NJ 08543

Phone: 609-243-2750
Fax: 609-243-2751
e-mail: pppl_info@pppl.gov
Internet Address: http://www.pppl.gov